NASA TM-80254

AN ACCURATE METHOD FOR COMPUTING THE ABSORPTION OF SOLAR RADIATION BY WATER VAPOR

by

Ming-Dah Chou and Albert Arking
Laboratory for Atmospheric Sciences
Goddard Space Flight Center
Greenbelt, MD 20771

April 1980

GODDARD SPACE FLIGHT CENTER
Greenbelt, Maryland

NASA TM-80254

AN ACCURATE METHOD FOR COMPUTING THE ABSORPTION OF SOLAR RADIATION BY WATER VAPOR

by

Ming-Dah Chou and Albert Arking
Laboratory for Atmospheric Sciences
Goddard Space Flight Center
Greenbelt, MD 20771

Abstract

A fast but accurate method has been developed to compute the absorption of solar radiation by water vapor. The method is based upon the molecular line parameters compiled by McClatchey et al., (1973), and makes use of the far-wing scaling approximation and k-distribution approach previously applied by Chou and Arking (1980) to the computation of the infrared cooling rate due to water vapor. Taking into account the wave number dependence of the incident solar flux, the solar heating rate is computed for the entire water vapor spectrum and for individual absorption bands. The accuracy of the method is tested against line by line calculations. Our method introduces a maximum error of 0.06°C/day, compared to Yamamoto's (1962) absorption curve, which introduces a maximum error of 0.25° C/day. The present method has the additional advantage over previous methods in that it can be applied to any portion of the spectral region containing the water vapor bands. We also compare the integrated absorptances and line intensities computed from the molecular line parameters with the laboratory measurements of Burch et al., (1965, 1966) and Ludwig (1971). The comparison reveals that, among the three different sources, absorptance is the largest for the laboratory measurements of Burch et al.

AN ACCURATE METHOD FOR COMPUTING THE ABSORPTION OF SOLAR RADIATION BY WATER VAPOR

1. Introduction

The increasing sophistication of numerical models of the atmosphere requires more accurate methods of treating radiative energy transport. At the same time, speed is essential, especially for the long term integration required in climate modelling. In a previous paper, Chou and Arking (1980) developed a fast but accurate method for computing the cooling rate in the infrared due to water vapor. Using a similar approach, this paper presents a method for computing the heating rates due to absorption of solar radiation by water vapor.

Most of the previous methods of modelling the molecular absorption of solar energy (e.g., McDonald, 1960; Manabe and Möller, 1961: Yamamoto, 1962; Sasamori et al., 1972) were based either on laboratory measurements or on direct solar radiation measurements. The laboratory measurements consist of transmittance through a cell containing a uniformly mixed gas at a fixed temperature and pressure, whereas the direct solar radiation measurements are made through an atmospheric slant path along which pressure, temperature, and humidity vary. In either case, the transformation to other paths and the calculation of transmittance are not straightforward. It is complicated by the large number of variables involved, including the high degree of variability in the water vapor distribution. It has been found that solar heating rates computed on the basis of these measurements could differ by nearly a factor of two (e.g., Wang, 1976) depending upon the methods used.

A further complication is the need to take into account atmospheric scattering by the molecular atmosphere and by cloud and aerosol particles. Since these molecular absorption measurements are made for wide spectral intervals, they cannot be applied directly to a scattering atmosphere, where the solution to the problem of multiple scattering in the atmosphere requires the monochronmatic values of the absorption coefficient. In order to apply the radiative transfer scheme including scattering, the transmittance within each spectral interval is approximated by an

exponential series, in which each term represents the transmittance associated with an equivalent absorption coefficient; the series coefficients and the equivalent absorption coefficients are empirically determined (Yamamoto et al., 1970; Lacis and Hansen, 1974; Liou and Sasamori, 1975). Although the representation of transmittance over a spectral interval as an exponential series (the so-called k-distribution method) is justified by theoretical considerations (Arking and Grossman, 1972), nonetheless, the empirical approach leads to a plethora of non-unique fits to the data. There is just not enough information in the wide spectral measurements to uniquely determine the distribution of absorption coefficients.

A far more preferable approach is the direct computation of transmittance from molecular line parameters. This is made possible by the extensive work in recent years to compile molecular line parameters for atmospheric gases (McClatchey, 1973). The most accurate method is a line-by-line computation along the spectrum. Because absorption is a rapidly varying function of wavenumber, the size of spectral interval required in a line-by-line computation is of the order of $0.01\,cm^{-1}$ or less. For repeated computations in an atmospheric model, the required computing time is far beyond what anyone can afford. Chou and Arking (1980) took advantage of the nature of atmospheric humidity distribution to develop an efficient method for computing transmittances in the infrared water vapor bands. The essence of that method is (1) to scale the absorption coefficient based on the conditions representative of the region in the atmosphere where cooling is most significant, and (2) to assume that the dependence of the absorption coefficient on temperature and pressure corresponds to that in the far wings of absorption lines. It leads to the separation of wave number dependence of transmittance from pressure and temperature and results in a one-parameter scaling. The k-distribution method (Arking and Grossman, 1972) can then be applied to the calculations of transmittance and flux in an inhomogeneous atmosphere, thereby greatly reducing computing time, but retaining a high degree of accuracy. In its final form, our method resembles the radiation routine of Lacis and Hansen (1974), which is based upon the absorption curve of Yamamoto (1962) and is used in the GLAS general circulation model. The essential differences are: (1) we compute the distribution of absorption coefficients

from molecular line parameters, instead of an exponential series fit to wide spectral measurements; and (2) the reference pressure for scaling the water vapor amount in our method is optimally selected instead of STP.

In this study, we extend the work of Chou and Arking (1980) to computing the absorption of solar radiation by water vapor. The validity of the method is verified by comparison with line-by-line calculations. The spectral region covered in this study is the region with wavelength longer than 0.86μm, which includes five water vapor bands. The weak 0.7 and 0.8μm bands are not included, since the molecular line parameters compiled by McClatchey et al., (1973) do not include these two bands. In Section 2, we outline an efficient method for transmittance and flux computations based upon actual line parameters. In Section 3, we compare the computed heating rate in clear atmospheres using the present method with that obtained from direct line-by-line calculations; comparison is also made with the Lacis and Hansen method, which is based on Yamamoto's absorption curve. Sample calculations for cloudy atmospheres are given in Section 4. In Section 5, band absorptances computed from line parameters and laboratory data are compared. A summary is presented in Section 6.

2. Formulation of the method

The parameters that affect the absorption coefficient are the line shape, intensity, and width. In the troposphere and lower stratosphere, the broadening of absorption lines is mainly due to molecular collision, and the absorption coefficient closely follows a Lorentz profile, with line width proportional to pressure. The effect of temperature on the absorption coefficient is mainly through its effect on line intensity. From line-by-line calculations, it has been found that for atmospheric conditions the absorption of solar radiation is significant only near the centers of absorption bands, where the temperature dependence is small. The effect of temperature on the absorption coefficient can therefore be neglected. The dependence of the absorption coefficient on pressure will be represented by a modification of the far-wing approximation used by Chou and Arking (1980) for the thermal infrared bands. Because the water vapor lines are weaker in

the solar spectral region, we here employ the approximation

$$k_\nu(p) = k_\nu(p_r, T_r) \left(\frac{p}{p_r}\right)^m, \tag{1}$$

where k is the absorption coefficient, ν wavenumber, p pressure, T temperature, and the subscript r denotes reference conditions. The parameter m should be somewhat less than 1 and is determined empirically.

Since our main concern is the transmittance between the top of the atmosphere and pressure levels within the atmosphere, p_r and T_r should represent conditions above the layers where most of the heating occurs. The reference temperature, being least important, was arbitrarily chosen to be 240K, and the reference pressure was empirically chosen to be 300mb. The parameter m, which should be close to 0 for weak absorption and 1 for strong absorption, was chosen to be 0.8. For this particular choice of reference pressure, the parameter m has the effect of reducing errors in the stratosphere and lower troposphere.

To compute the absorption of solar energy, we start with spectral intervals $\Delta\nu_i$, i = 1, . . . n, such that the solar energy incident at the top of the atmosphere can be considered constant within each spectral interval. The solar flux at pressure level p is

$$\mu F(p) = \mu \sum_{i=1}^{n} F_i(0)\, \tau_i(p)\, \Delta\nu_i, \tag{2}$$

where $\mu F_i(0)\Delta\nu_i$ is the incoming solar energy at the top of the atmosphere, $\tau_i(p)$ is the mean transmittance between the top of the atmosphere and pressure level p, given by

$$\tau_i(p) = \int_{\Delta\nu_i} \exp\left[-\frac{1}{\mu g}\int_0^p k_\nu(p',T)\, q(p')dp'\right] d\nu \Big/ \Delta\nu_i \tag{3}$$

q is specific humidity, g the acceleration of gravity, and μ cosine of the solar zenith angle. To take advantage of approximation (1), we let $h_i(k)$ represent the distribution of the absorption coefficient $k_\nu(p_r,T_r)$ within the spectral interval, with the normalization

$$\int_{k_{min}}^{k_{max}} h_i(k)\, d\log k = 1,$$

where k_{min} and k_{max} are the minimum and maximum values, respectively, of $k_\nu(p_r,T_r)$ within the spectral interval. This allows us to transform (3) into

$$\tau_i(p) = \int_{k_{min}}^{k_{max}} \exp\,[-kw(p)/\mu]\; h_i(k)\, d\log k \tag{4}$$

where w(p) is the scaled water vapor amount,

$$w(p) = \frac{1}{g}\int_o^p \left(\frac{p'}{p_r}\right)^m q(p')\, dp'. \tag{5}$$

With the substitution of (4), Eq. (2) becomes

$$\mu F(p) = \mu \int \exp\,[-kw(p)/\mu]\; h(k)\, d\log k \tag{6}$$

where h(k) is the weighted k-distribution function, defined by

$$h(k) = \sum_{i=1}^{n} F_i(0)\, \Delta\nu_i\, h_i(k)$$

We compute the k-distribution functions by first computing the absorption coefficient $k_\nu(p_r,T_r)$, with p_r = 300mb and T_r=240k, using a Voight line profile and the line parameters compiled by McClatchey et al., (1973). The computations are carried out over the spectral range 2600–12040cm^{-1}. The spectrum is divided into 236 spectral intervals of 40cm^{-1} each, and they include the five water vapor absorption bands listed in Table 1. Since water vapor lines with wave number greater than 12040cm^{-1} were not available, the weak 0.7 and 0.8μm bands are not included in this study. The solar flux outside the atmosphere $F_i(0)$ is taken from Labs and Neckel (1968).

The weighted k-distribution function h(k) is computed separately for each of the water vapor absorption bands and for the total spectrum; it is shown in Table 2. The total solar flux μF at any point in the atmosphere, integrated over the entire spectrum, is a function of the solar zenith angle and the scaled water vapor amount above that point. Values of $F(w/\mu)$ are shown in Table 3.

3. Heating rate in a clear atmosphere

a. Test of the wing scaling approximation. To test the accuracy of the wing scaling approximation, two sets of heating rates have been computed, based upon line-by-line calculations of

transmittance and flux every $0.02\,cm^{-1}$. In one set, the absorption coefficient is computed from the line parameters for a Voigt line shape which varies with height according to the temperature and pressure profiles of the model atmosphere; this represents the "exact" calculation. In the second set, we proceed as in the first set but substitute the wing scaling approximation given by (1) for the variation of the absorption coefficient with height (with p_r = 300mb, T_r = 240K, and m = 0.8). In each set, the heating rate for any atmospheric layer is proportional to the difference in fluxes at the top and bottom of the layer, with flux computed using the transmittance given by (3). The results are shown in Figs. 1a–f for a clear, mid-latitude winter atmosphere, with a solar zenith angle of 60° and zero surface albedo. It can be seen that in each band the error due to the wing scaling approximation is <0.015°C/day below 50mb; in the worst case, the 0.94μm band, the error is less than 7% of the peak heating rate due to that band. For the total heating rate due to the combined spectrum (Fig. 1f), the error below 50mb is <0.025°C/day, which is less than 2.5% of the peak heating rate.

The errors can be understood as follows. In the stratosphere, where $p < p_r$, the wing scaling approximation underestimates the absorption. Hence, more energy is available in the upper troposphere and the heating rate there is overestimated. In the lower troposphere, because of the long optical path, the band wings are relatively more important. Since absorption in the band wings increases with increasing temperature, the heating rates are underestimated wherever the temperature is higher than the reference temperature of 240K.

b. The fast method. In order to achieve the high speed necessary for repeated computations in numerical models of the atmosphere, the scaled water vapor amount is computed using (5) and the flux computed from (6). In practice $F(w/\mu)$ is stored and a table lookup procedure is used (Table 3).

Examples showing the accuracy of the fast method appear in Figs. 2–4. "Exact" calculations of the solar heating rate are shown in Fig. 2 for two model atmospheres: mid-latitude winter and tropical. The differences in claculated heating rates between the fast and "exact" methods are shown in Figs. 3 and 4. Also shown, for comparison, are the differences from the "exact" when

using the formula of Lacis and Hansen (1974), which is based on Yamamoto's (1962) absorption curve. For Yamamoto's heating rate profiles (dashed curves), the scaled water vapor amount is computed from (5) with p_r = 1013 mb.

It can be seen from Figs. 3 and 4 that differences between the heating rates using the present method and the line-by-line method are small, with a maximum of 0.06°C/day. This good agreement arises partly from the fact that they are obtained using the same set of absorption parameters compiled by McClatchey et al., (1973), but at the same time, it shows the validity of the wing scaling approximation. The differences between the heating rates using Yamamoto's absorption curve and the line-by-line method are about 3 to 4 times larger than for the present method. Part of the discrepancies can be traced to the use of different sets of absorption data. The "exact" heating rate is computed from line parameters, while Yamamoto's absorption curve is derived from the laboratory measurements of Howard et al., (1956) and the solar radiation measurements of Fowle (1915). Also, the choice of the standard pressure as the reference pressure for water vapor scaling is believed to account for a substantial part of these discrepancies. It is clear that line center portions of the spectrum are important to the absorption of solar energy in the stratosphere and upper troposphere because of the small optical depth there. When water vapor is scaled linearly with pressure based on the standard pressure, the absorption in line center portions are greatly underestimated. This can be seen in Figs. 3 and 4 that Yamamoto's heating rates above the 300 mb level are much smaller than the "exact" ones. The heating rate error in the upper troposphere and stratosphere can be reduced by changing the value of the scaling parameter m from 1 to, say, 0.5, but then the heating rate errors in the middle and lower troposphere would be increased since the value of the scaling parameter in these parts of the atmosphere should be close to 1 (see Fig. 5). Comparing Fig. 3 with Fig. 5, it can be seen that the overall errors in heating rate cannot be reduced by changing the value of the scaling parameter m. It should be noted that Yamamoto's heating rates include absorption in the 0.7 and 0.8 μm bands, which we have neglected. However, the effect of these bands on solar heating is believed to be sufficiently small, especially for the drier atmosphere (cf. Fig. 1 of Yamamoto, 1962), that our conclusion is unaffected.

Table 4 shows the absorption of solar energy in the 2600–12040 cm^{-1} spectral region by the entire air column computed from the different methods. The present method is in fairly good agreement ($\lesssim 2\%$) with the line-by-line calculations for both the mid-latitude winter and tropical atmospheres. The calculations based upon Yamamoto's absorption data are within 6% of the line-by-line calculations.

4. Heating rate in a cloudy atmosphere

In addition to clear atmospheres, we also like to justify the use of the wing scaling approximation in cloudy atmospheres. Although there are several methods available for computing radiation terms including scattering, we have chosen the delta-Eddington approximation (Joseph et al., 1976; Wiscombe, 1977) to compute solar heating rate in cloudy atmospheres. In applying the delta-Eddington approximation, we divide the atmosphere into 20 layers with the thickness of each layer equal to 50mb. A cloud is assumed to be in the layers between the 500 and 600mb levels with a scattering optical depth equal to 20. This cloud can be considered as an altostratus or altocumulus. The cloud asymmetry factor necessary for the flux computations is assigned to be 0.85 which is a typical mean value for all clouds and wavenumbers (Hansen and Pollack, 1970). The relative humidity within the cloud is assumed to be 100%, and the surface albedo and solar zenith angle are set to be 0.07 and 60°, respectively. Since our purpose is to test the validity of the wing scaling approximation but not the absorption by cloud droplets which is not well known, the absorption of solar radiation by cloud droplets is not included.

The computed heating rate profiles using the present method are compared with those using the "exact" line-by-line method and Yamamoto's absorption curve. For the heating rate computations using the present method, we first compute fluxes for each k using the delta-Eddington approximation with w computed from (5) and the incoming solar energy normalized to 1. The total flux is then the sum of these fluxes multiplied by $\mu h(k)\, d\log k$ as indicated in (6). To apply Yamamoto's absorption curve to the scattering scheme which is derived for a monochromatic case, the mean absorption function is reduced to a form equivalent to (4) (e.g., Yamamoto et al., 1970; Lacis and Hansen, 1974; Liou and Sasamori, 1975) as

$$\tau_i(w) = \sum_{n=1}^{N} a_n \exp(-b_n w) \tag{7}$$

where a_n and b_n are obtained using a least square fit, w is given by (5) with p_r = 1013 mb, and N is the number of terms used to fit τ_i. Total fluxes are computed similar to the procedures just described for the case using the present method.

Comparisons of the present methods (using Table 2) with line-by-line methods are made in Fig. 6 for the 0.94 and 1.38 μm bands. It can be seen that the results of the present method are in good agreement with the line-by-line calculations. The difference is less than 0.015°C/day except at the top layer where the difference is 0.03°C/day for the 1.38 μm band.

Two heating rate profiles computed from the present method and using Yamamoto's absorption curve are compared in Fig. 7. The weighted k-distribution function listed in the last column of Table 2 is used for the present method, and the coefficients a_n and b_n obtained by Lacis and Hansen (1974) are used for the case using Yamamoto's absorption curve. It can be seen that these two heating rate profiles agree well except in the region above the 300 mb level where the maximum difference is 0.13°C/day. The underestimation and overestimation of Yamamoto's heating rate, respectively, above the 300 mb level and in the lower troposphere agree with the result shown in Fig. 4 for the clear case. However, the mean column heating rate using Yamamoto's absorption curve (0.39°C/day) is slightly less than that using the present method (0.41°C/day), which is contrary to the results for the clear cases (see Table 4). This is an indication of the uncertainty arising from the use of an exponential series fit to mean transmission functions.

5. Comparison of absorption data

In a study to parameterize the absorption of solar radiation by water vapor in the earth's atmosphere, Wang (1976) computed the heating rate profiles using several different absorption data. It has been found that the clear atmospheric heating rates computed with different methods could differ by as much as 40% of the peak heating rate. Among the different methods, the use of Yamamoto's absorption curve gives the largest absorption. We have computed the heating rate

profiles using the line-by-line method for the same clear atmospheres as used in Wang (1976) and found that the heating rate computed with the line-by-line method is larger than any of the other methods except the one using Yamamoto's absorption curve. Since these discrepancies are believed to arise primarily from the use of different absorption data, it is our purpose in this section to compare the absorption data derived from laboratory measurements and absorption line parameters.

Table 5 lists the integrated line intensities over each water vapor band computed from the line parameters compiled by McClatchey et al., (1973) together with the laboratory results of Burch et al., (1965, 1966) and Ludwig (1971). The integrated line intensities from the three different sources are in good agreement for the 1.87, and 2.7μm bands. For the 1.14 and 1.38μm bands, Ludwig's data give too weak absorption compared to the other two. Except for the 1.14 μm band, the integrated line intensities computed from the line parameters are smaller than the laboratory results of Burch et al.

The intensity of individual lines in an absorption band covers a range of several orders of magnitude, and the integrated line intensities shown in Table 5 are dominated by strong lines in the center of each absorption band. Since lines with medium intensity are also important to the absorption of solar energy, we need to know the absorption as a function of wave number in order to assess the possible effects on the solar heating of the atmosphere computed from different absorption data. Fig. 8 shows the integrated absorptance computed from line parameters and Burch's laboratory data for the 1.14, 1.38, and 1.87μm bands. The integrated absorptance, $A(\nu)$, is defined as

$$A(\nu) = \int_{\nu_1}^{\nu} A'(\nu')d\nu', \tag{11}$$

where $A'(\nu)$ is the absorptance at ν, and ν_1 is the starting wave number. The curves of $A(\nu)$ shown in Fig. 8 are for a homogeneous path with water vapor amount equal to 0.0411 g/cm^2, p = 305 mb, and T = 296 K. It can be seen that except for the 1.14μm band the absorptances derived from the line parameters and the laboratory measurements do not agree well. The laboratory

results give larger band absorptions as compared to the theoretical computations. The discrepancy is about 15% for the 1.38 and 1.87μm bands.

6. Summary

A method has been developed for computing the absorption of solar radiation by atmospheric water vapor. It is based upon line parameter data with accuracy comparable to that of line-by-line calculations. High speed is achieved by using a one-parameter scaling approximation to convert an inhomogeneous path into an equivalent homogeneous path at suitably chosen reference conditions (p_r = 300mb and T_r = 240K). Pre-computed tables (based upon line-by-line calculations) of either the absorption coefficient distribution (i.e., k-distribution) or the transmittance of solar flux versus equivalent water vapor amount, both of which are tabulated, provide the user with a fast method suitable for climate models or general circulation models. The variation of incident solar flux with wavenumber within the water vapor absorbing region (2600-12040cm^{-1}) has been folded into the tables.

The present method is similar in form and speed to that of Lacis and Hansen (1974). It differs primarily in that (1) their transmittances are based upon the empirically derived absorption curve of Yamamoto (1962) whereas we use the line parameter data of McClatchey et al., (1973), and (2) their water vapor amount is scaled to STP whereas we use upper tropospheric values (300mb and 240K).

The accuracies of the present method and of the method based on Yamamoto's absorption curve are compared to line-by-line calculations for two clear model atmospheres: Mid-latitude winter and tropical. The present method has a maximum error of 0.06°C/day, which is less than 5% of the peak heating rate. The Yamamoto method has a maximum error of 0.25°C/day.

The method has also been applied to the case of a cloudy atmosphere, using the delta-Eddington approximation (Joseph et al., 1976) to account for multiple scattering within the cloud. This example illustrates the very strong influence that clouds have on the vertical distribution of solar heating in the atmosphere.

The present method has the additional advantage over previous methods in that it can be applied to any portion of the spectral region containing the water vapor bands. It thus permits one to take into account the combined effects of aerosols or trace gases that may alter the spectral distribution of solar energy reaching the water vapor layer.

Acknowledgments

The authors are grateful to Dr. J. Joseph for valuable comments and to Dr. W. Wiscombe for providing listings of the computer code for the delta-Eddington approximation.

7. References

Arking, A., and K. Grossman, 1972: The influence of line shape and band structure on temperatures in planetary atmosphere. J. Atmos. Sci., 29, 937-949.

Burch, D. E., D. A. Gryvnak, and R. R. Patty, 1965: Absorption by H_2O between 2800 and 4500 cm^{-1} (2.7 micron region). Aeronutronic Rept. U-3202. [NTIS 66N 35108]

Burch, D. E., and D. A. Gryvnak, 1966: Absorption by H_2O between 5045-14 485 cm^{-1} (0.69-1.98 microns). Aeronutronic Rept. U-3704. [NTIS 68N 12574]

Chou, M.-D., and A. Arking, 1980: Computation of infrared fluxes in the water vapor bands. To appear in J. Atmos. Sci., April issue.

Fowle, F. E., 1915: The transparency of aqueous vapor. Astrophys. J., 42, 394-411.

Hansen, J. E., and J. B. Pollack, 1970: Near infrared light scattering by terrestrial clouds. J. Atmos. Sci., 27, 265-281.

Howard, J. N., D. E. Burch, and D. Williams, 1956: Infrared transmission of synthetic atmospheres III. Absorption of water vapor. J. Opt. Soc., Amer., 46, 242-245.

Joseph, J. H., W. J. Wiscombe, and J. A. Weinman, 1976: The delta-Eddington approximation for radiative flux transfer. J. Atmos. Sci., 33, 2452-2459.

Labs, D., and H. Neckel, 1968: The radiation of the solar photosphere from 2000 A to 100μ. Zeitschrift für Astrophysik, 69, 1-73.

Lacis, A. A., and J. E. Hansen, 1974: A parameterization for the absorption of solar radiation in the Earth's atmosphere. J. Atmos. Sci., 31, 118-133.

Liou, K. N., and T. Sasamori, 1975: On the transfer of solar radiation in aerosol atmosphere. J. Atmos. Sci., 32, 2166-2177.

Ludwig, C. B., 1971: Measurement of the curves-of-growth of hot water vapor. Appl. Optics., 10, 1057-1033.

McClatchey, R. A., W. S. Benedict, S. A. Clough, D. E. Burch, R. F. Calfee, K. Fox, L. S. Rothman, and J. S. Garing, 1973: AFCRL atmospheric absorption line parameters compilation. Environ. Res. Pap., No. 434, AFCRL-TR-73-0096. [NTIS AD 762904]

Manabe, S., and F. Möller, 1961: On the radiative equilibrium and heat balance of the atmosphere. Mon. Wea. Rev., 89, 503-532.

McDonald, J. E., 1960: Direct absorption of solar radiation by atmospheric water vapor. J. Meteor., 17, 319-328.

Sasamori, T., J. London, and D. V. Hoyt, 1972: Radiation budget of Southern Hemisphere. Meteor. Monogra., 13, No. 35, 9-23.

Wang, W.-C., 1976: A parameterization for the absorption of solar radiation by water vapor in the earth's atmosphere. J. Appl. Meteor., 15, 21-27.

Wiscombe, W. J., 1977: The delta-Eddington approximation for a vertically inhomogeneous atmosphere. NCAR/TN-121 STR, NCAR Tech. Note, pp. 66.

Yamamoto, G., 1962: Direct absorption of solar radiation by atmospheric water vapor, carbon dioxide and molecular oxygen. J. Atmos. Sci., 19, 182-188.

Yamamoto, G., M. Tanaka, and S. Asano, 1970: Radiative transfer in water clouds in the infrared region. J. Atmos. Sci., 27, 282-292.

Table 1
Spectral range of absorption bands.

Absorption Band (μm)	Spectral Range (cm^{-1})
0.94	9600–11600
1.14	8200– 9600
1.38	6300– 8200
1.87	4400– 6300
2.7	2600– 4400
Total	2600–12040

Table 2
Weighted k-distribution function, h (mW/cm^2), with p_r = 300mb, T_r = 240K.
k(g^{-1} cm^2) is the absorption coefficient.

Log k	0.94μm	1.14μm	1.38μm	1.87μm	2.7μm	Total
-5.000	8.605	4.021	5.246	5.692	0.081	25.032
-4.700	2.053	0.432	1.295	0.764	0.077	5.153
-4.400	2.380	0.596	1.440	0.962	0.172	6.198
-4.100	2.515	0.598	1.498	1.168	0.187	6.979
-3.800	1.985	0.769	1.533	1.337	0.236	7.023
-3.500	1.618	0.830	1.562	1.493	0.273	6.762
-3.200	1.615	1.155	1.573	1.935	0.318	7.721
-2.900	1.756	1.832	1.425	1.722	0.480	8.118
-2.600	2.471	2.442	1.478	1.500	0.589	9.338
-2.300	3.071	2.686	1.623	1.523	0.774	10.287
-2.000	3.346	2.524	1.366	1.406	0.835	9.902
-1.700	3.557	2.501	1.447	1.197	0.845	9.864
-1.400	3.278	2.478	1.838	1.051	0.933	9.798
-1.100	2.886	2.478	2.097	1.051	0.979	9.654
-0.800	2.397	2.264	2.340	0.916	0.998	9.020
-0.500	1.723	1.856	2.468	1.003	0.945	8.061
-0.200	1.223	1.325	2.428	1.197	0.823	7.022
0.100	0.841	0.910	2.446	1.288	0.762	6.259
0.400	0.558	0.635	2.112	1.249	0.710	5.271
0.700	0.385	0.434	1.828	1.054	0.737	4.439
1.000	0.237	0.270	1.420	0.802	0.777	3.507
1.300	0.137	0.166	1.010	0.613	0.744	2.671
1.600	0.078	0.110	0.701	0.441	0.670	2.000
1.900	0.044	0.081	0.455	0.285	0.536	1.401
2.200	0.022	0.053	0.297	0.202	0.383	0.957
2.500	0.002	0.024	0.193	0.133	0.286	0.638
2.800	0.0	0.004	0.112	0.091	0.187	0.394
3.100	0.0	0.0	0.080	0.064	0.124	0.268
3.400	0.0	0.0	0.034	0.040	0.084	0.157
3.700	0.0	0.0	0.018	0.024	0.134	0.176

Table 3

Transmitted solar flux F in the spectral range 2600–12040 cm^{-1}, in mW/cm^2, as a function of w/μ, where w is the scaled water vapor amount in g/cm^2 and μ is the cosine of the solar zenith angle. The solar flux at the top of the atmosphere is taken to be 55.217 mW/cm^2.

Log w/μ	F	Log w/μ	F
-4.0	55.141	-1.2	51.493
-3.9	55.126	-1.1	51.107
-3.8	55.108	-1.0	50.693
-3.7	55.087	-0.9	50.251
-3.6	55.063	-0.8	49.780
-3.5	55.036	-0.7	49.280
-3.4	55.004	-0.6	48.751
-3.3	54.967	-0.5	48.193
-3.2	54.924	-0.4	47.605
-3.1	54.876	-0.3	46.989
-3.0	54.820	-0.2	46.343
-2.9	54.757	-0.1	45.669
-2.8	54.686	-0.0	44.967
-2.7	54.605	0.1	44.238
-2.6	54.513	0.2	43.481
-2.5	54.411	0.3	42.697
-2.4	54.295	0.4	41.888
-2.3	54.166	0.5	41.054
-2.2	54.022	0.6	40.196
-2.1	53.862	0.7	39.316
-2.0	53.684	0.8	38.416
-1.9	53.488	0.9	37.499
-1.8	53.271	1.0	36.566
-1.7	53.034	1.1	35.621
-1.6	52.775	1.2	34.666
-1.5	52.492	1.3	33.703
-1.4	52.184	1.4	32.736
-1.3	51.852		

Table 4
Absorption of solar energy (mW/cm^2) by water vapor with solar zenith angle equal to 60° and surface albedo equal to zero. Numbers in parentheses are the heating rate (°C/day) of the entire air column.

	Line-by-Line Method	Present Method	Yamamoto (1962)	
			m = 0.5	m = 1.0
Tropical	10.56 (0.892)	10.47 (0.884)	11.43 (0.965)	11.17 (0.943)
Mid-Latitude Winter	7.12 (0.601)	7.27 (0.615)	7.23 (0.612)	7.51 (0.634)

Table 5
Integrated line intensity (g^{-1} cm) of water vapor absorption bands at room temperature.

	0.94μm	1.14μm	1.38μm	1.87μm	2.7μm
McClatchey et al., (1973)	8.87×10^2	1.76×10^3	2.51×10^4	3.09×10^4	2.76×10^5
Burch et al., (1965, 1966)	$(9.84 \pm 0.5) \times 10^2$ *	$(1.16 \pm 0.08) \times 10^3$	$(2.55 \pm 0.13) \times 10^4$	$(3.16 \pm 0.16) \times 10^4$	$(2.84 \pm 0.16) \times 10^5$
Ludwig, (1971)	–	22.3	1.58×10^4	3.33×10^4	2.68×10^5

*T = 443k

FIGURE CAPTIONS

Fig. 1a. Solar heating rates in the 0.94μm band computed from the line-by-line method for the solar zenith angle of 60° and zero ground albedo. The solid curve is computed by taking the pressure and temperature effects on absorption exactly into account. The dashed curve is computed using the wing scaling approximation of (1).

Fig. 1b. Same as Fig. 1a except for the 1.14μm band.

Fig. 1c. Same as Fig. 1a except for the 1.38μm band.

Fig. 1d. Same as Fig. 1a except for the 1.87μm band.

Fig. 1e. Same as Fig. 1a except for the 2.7μm band.

Fig. 1f. Same as Fig. 1a except for the 2600–12040cm^{-1} spectral region.

Fig. 2. Solar heating rates computed from exact line-by-line methods for a clear tropical atmosphere and a mid-latitude winter atmosphere. The solar zenith angle and surface albedo are set at 60° and 0, respecticely.

Fig. 3. Errors of the computed heating rates for a clear tropical atmosphere. The solid and dashed curves correspond, respectively, to cases using Table 3 and Yamamoto's (1962) absorption curve.

Fig. 4. Same as Fig. 3 except for a clear mid-latitude winter atmosphere.

Fig. 5. Same as Fig. 3 except the scaling parameter for Yamamoto is set to be 0.5.

Fig. 6. Computed heating rate profiles due to water vapor absorption in the 0.94 and 1.38μm bands. Calculations were made for a cloudy mid-latitude winter atmosphere with a solar zenith angle of 60° and a zero surface albedo.

Fig. 7. Computed heating rate profiles due to water vapor absorption in the 2600–12040 cm^{-1} region. Calculations were made for a cloudy mid-latitude winter atmosphere with a solar zenith angle of 60° and a zero surface albedo.

Fig. 8. Integrated absorptances for a homogeneous path at p = 305 mb, T = 296 K with a water vapor content of 0.0041 g/cm^2. For convenience, the wave numbers where the integration starts are reduced to zero. The actual starting wave numbers are 8560, 6640, and 5040 cm^{-1} for the 1.14, 1.38, and 1.87 μm bands, respectively.

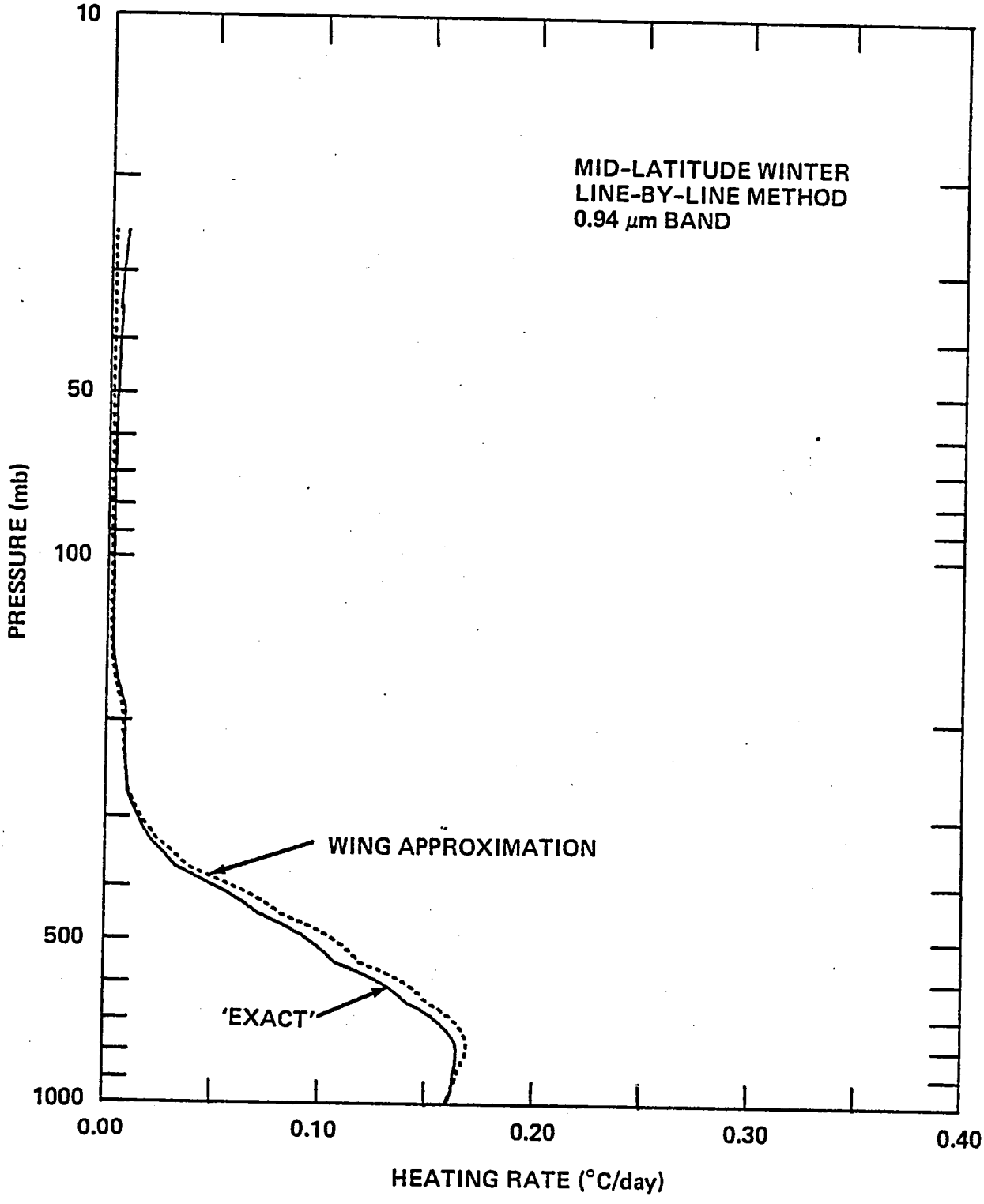
10
50
100
500
1000
PRESSURE (mb)
MID-LATITUDE WINTER
LINE-BY-LINE METHOD
0.94 μm BAND
WING APPROXIMATION
'EXACT'
0.00
0.10
0.20
0.30
0.40
HEATING RATE (°C/day)

Fig. 1a

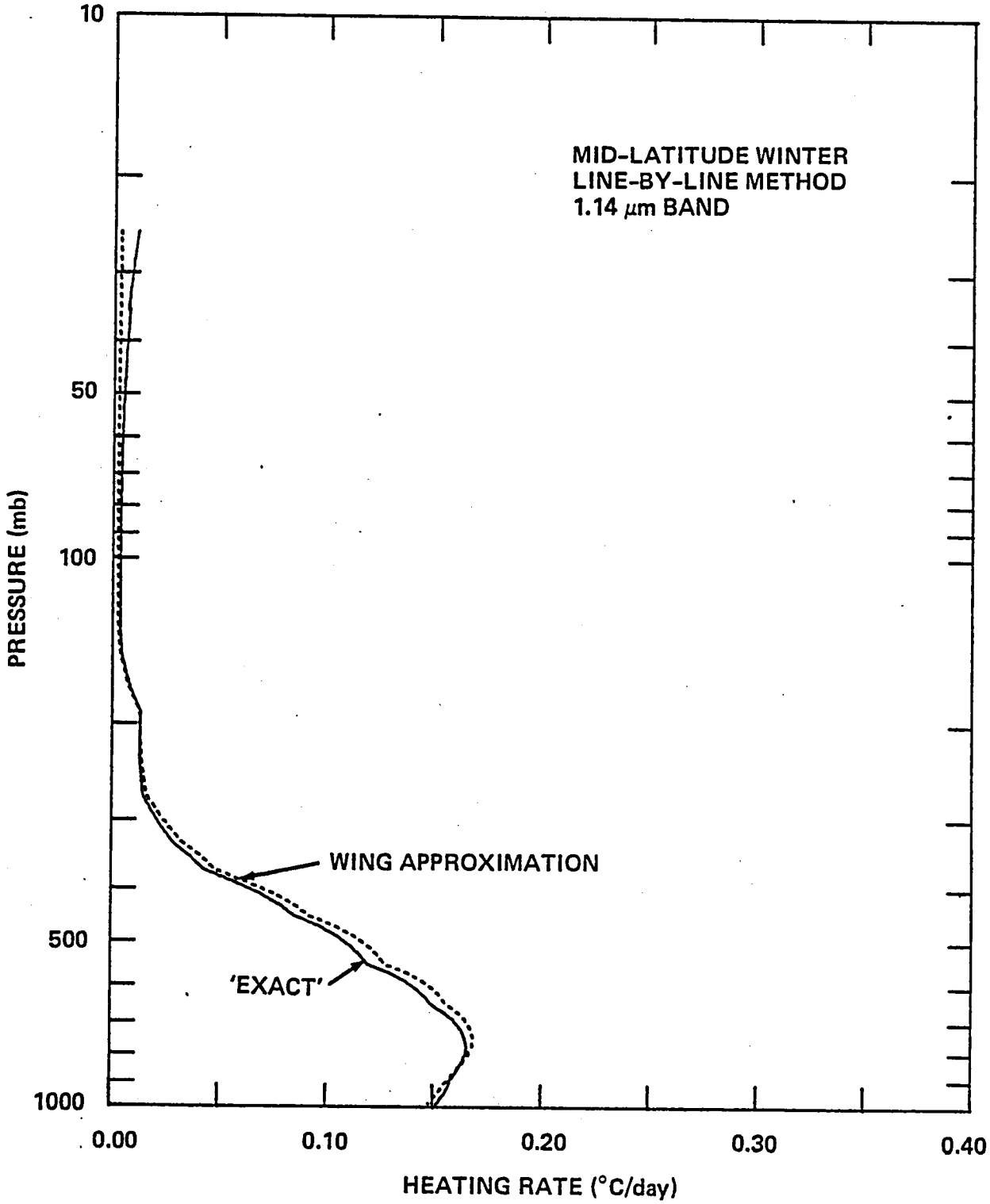
MID-LATITUDE WINTER
LINE-BY-LINE METHOD
1.14 μm BAND
WING APPROXIMATION
'EXACT'
PRESSURE (mb)
10
50
100
500
1000
0.00
0.10
0.20
0.30
0.40
HEATING RATE (°C/day)

Fig. 1b

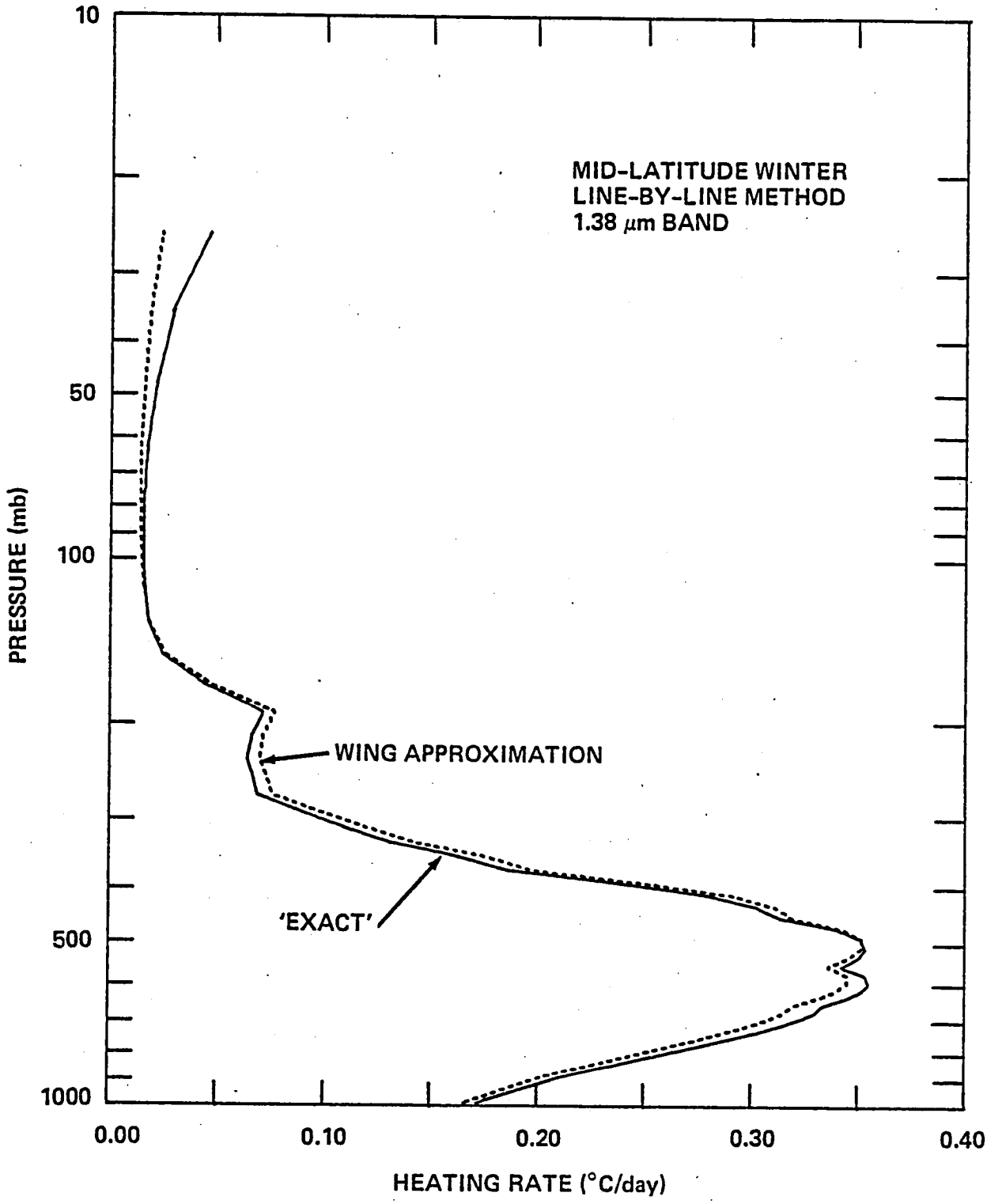
MID-LATITUDE WINTER
LINE-BY-LINE METHOD
1.38 μm BAND
WING APPROXIMATION
'EXACT'
PRESSURE (mb)
10
50
100
500
1000
0.00
0.10
0.20
0.30
0.40
HEATING RATE (°C/day)

Fig. 1c

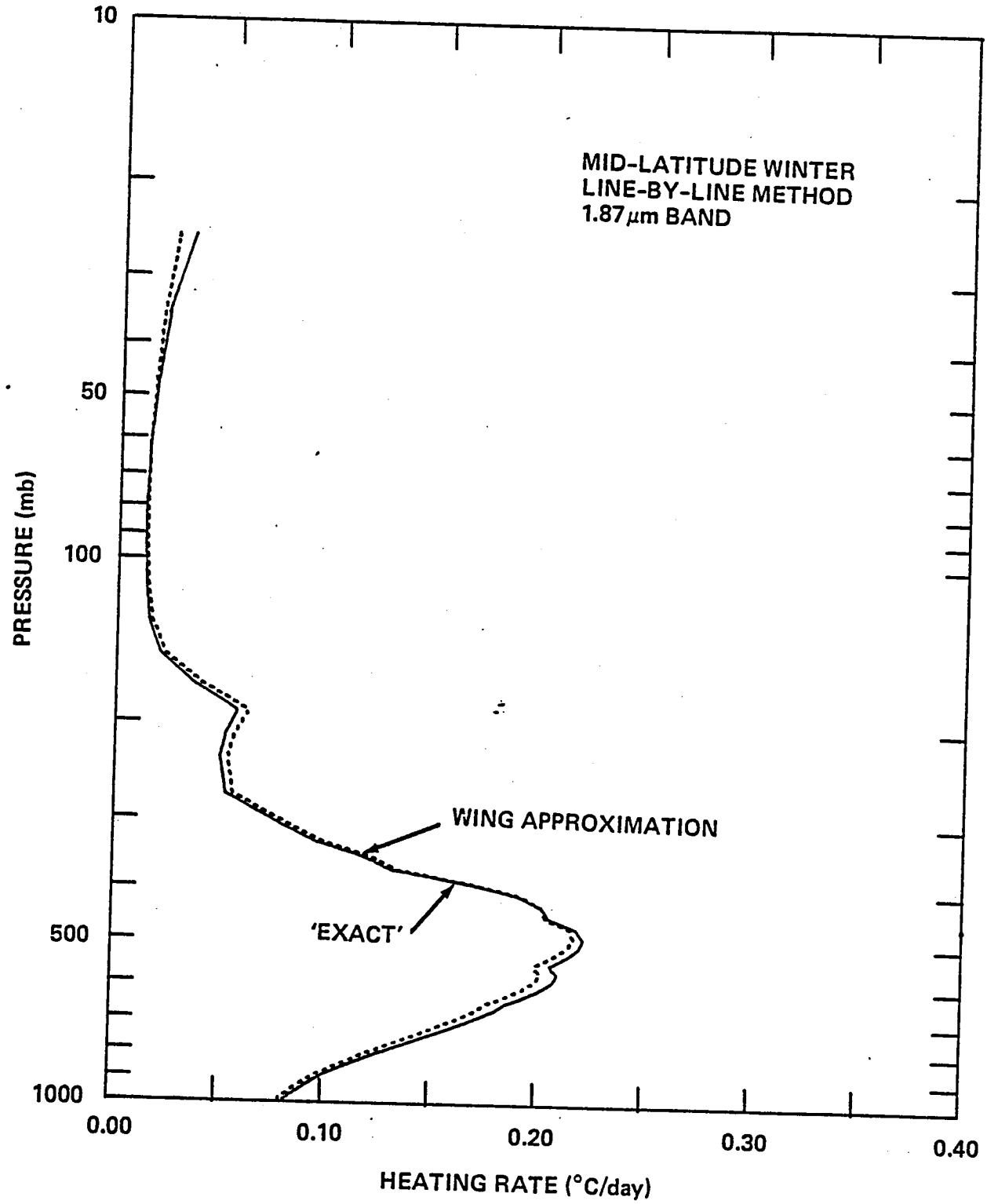
MID-LATITUDE WINTER
LINE-BY-LINE METHOD
1.87 μm BAND
WING APPROXIMATION
'EXACT'
PRESSURE (mb)
10
50
100
500
1000
0.00
0.10
0.20
0.30
0.40
HEATING RATE (°C/day)

Fig. 1d .

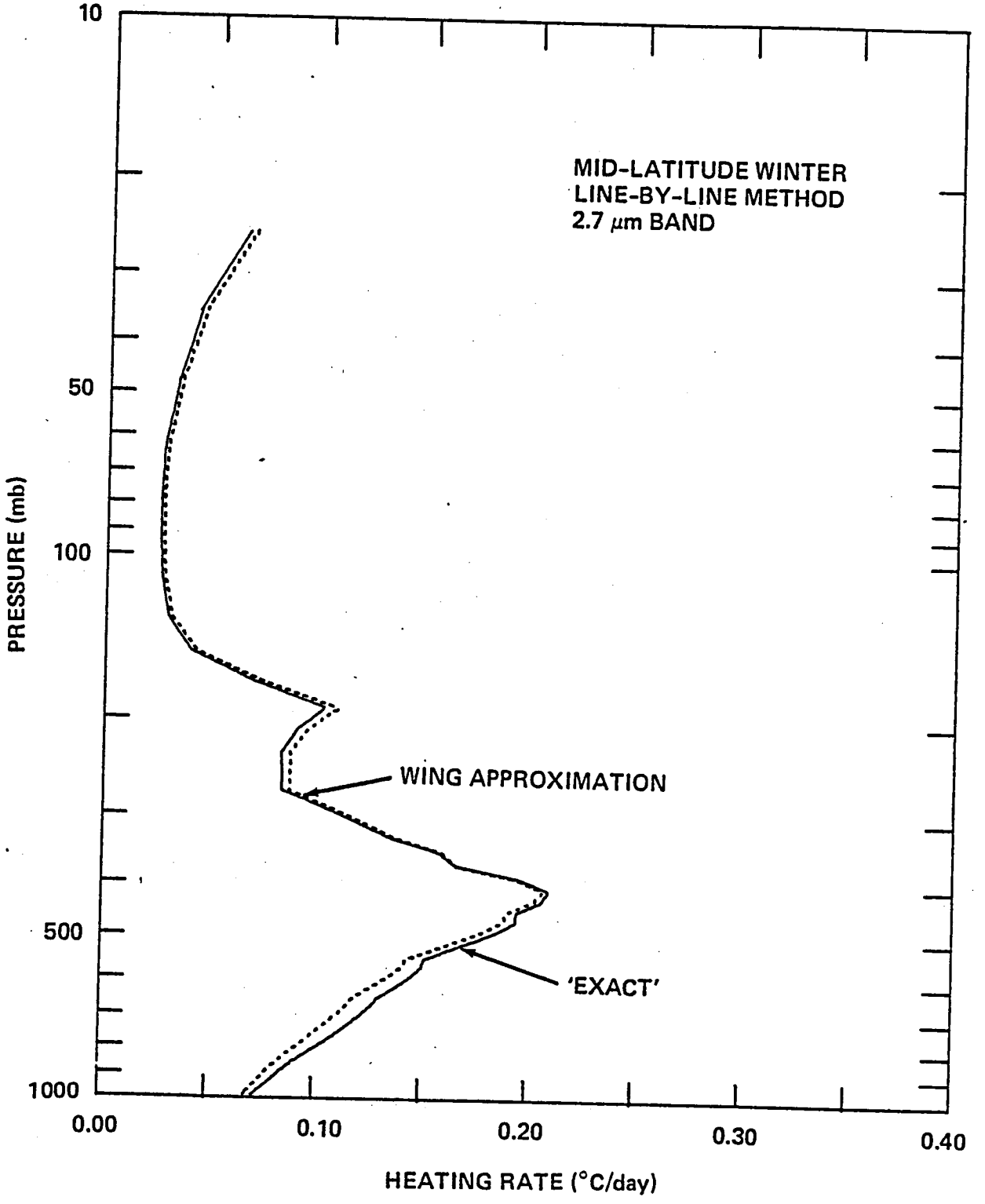
MID-LATITUDE WINTER
LINE-BY-LINE METHOD
2.7 μm BAND
WING APPROXIMATION
'EXACT'
PRESSURE (mb)
10
50
100
500
1000
0.00
0.10
0.20
0.30
0.40
HEATING RATE (°C/day)

Fig. 1e

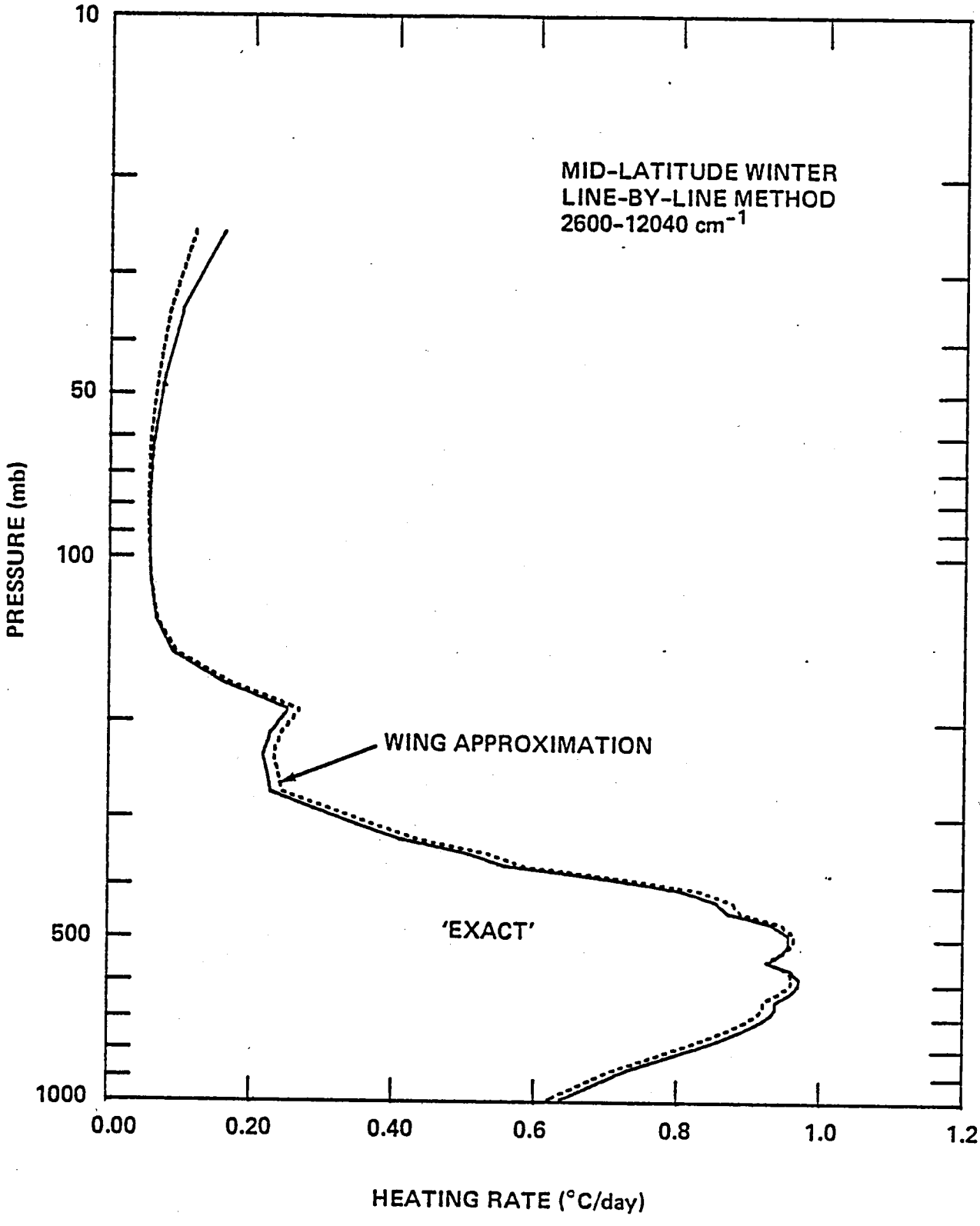
MID-LATITUDE WINTER
LINE-BY-LINE METHOD
2600-12040 cm^{-1}
WING APPROXIMATION
'EXACT'
PRESSURE (mb)
10
50
100
500
1000
0.00
0.20
0.40
0.6
0.8
1.0
1.2
HEATING RATE (°C/day)

Fig. 1f

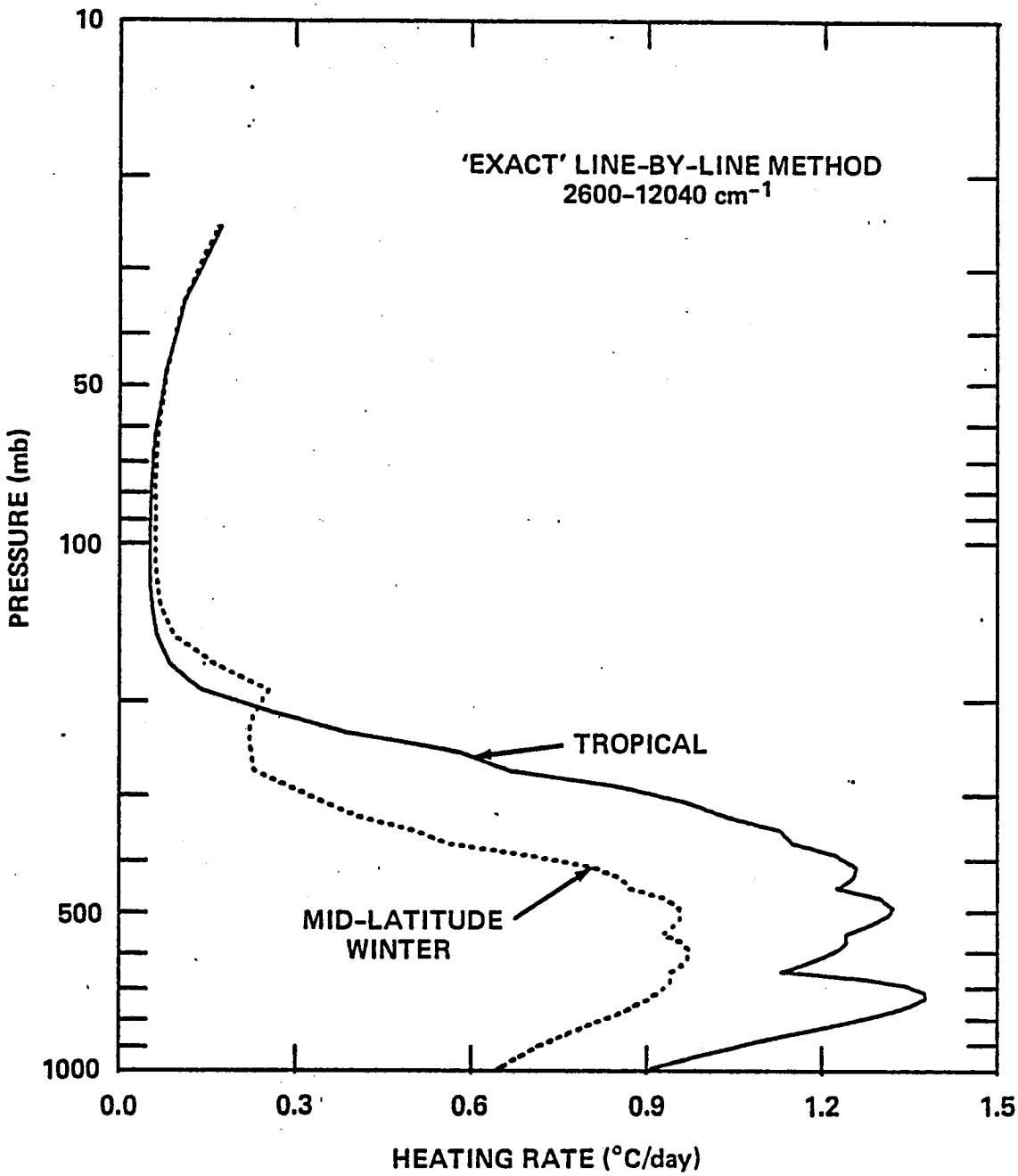
'EXACT' LINE-BY-LINE METHOD
2600–12040 cm⁻¹
TROPICAL
MID-LATITUDE
WINTER
PRESSURE (mb)
10
50
100
500
1000
0.0
0.3
0.6
0.9
1.2
1.5
HEATING RATE (°C/day)

Fig. 2

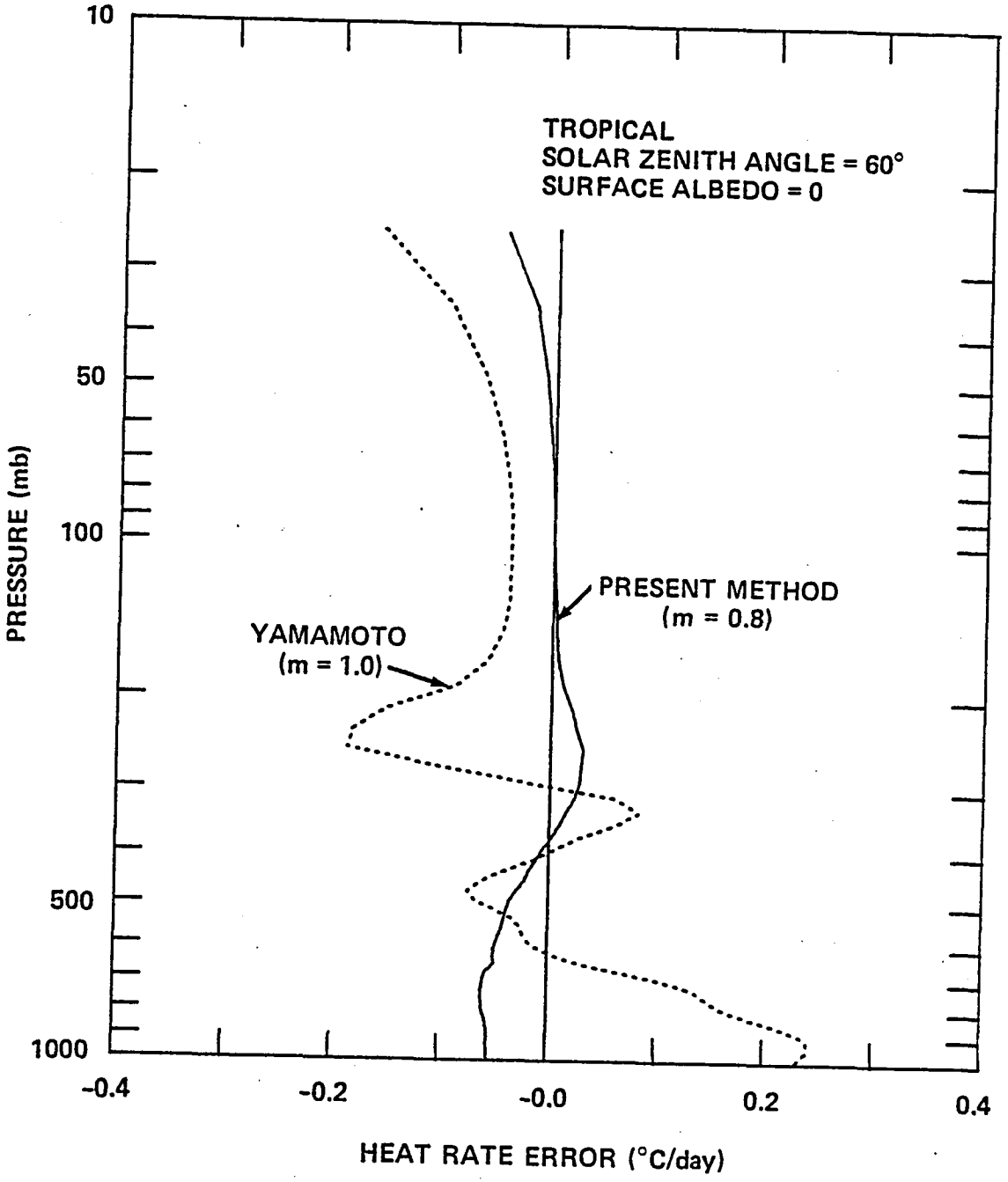
10
50
100
500
1000
PRESSURE (mb)
TROPICAL
SOLAR ZENITH ANGLE = 60°
SURFACE ALBEDO = 0
YAMAMOTO
(m = 1.0)
PRESENT METHOD
(m = 0.8)
-0.4
-0.2
-0.0
0.2
0.4
HEAT RATE ERROR (°C/day)

Fig. 3

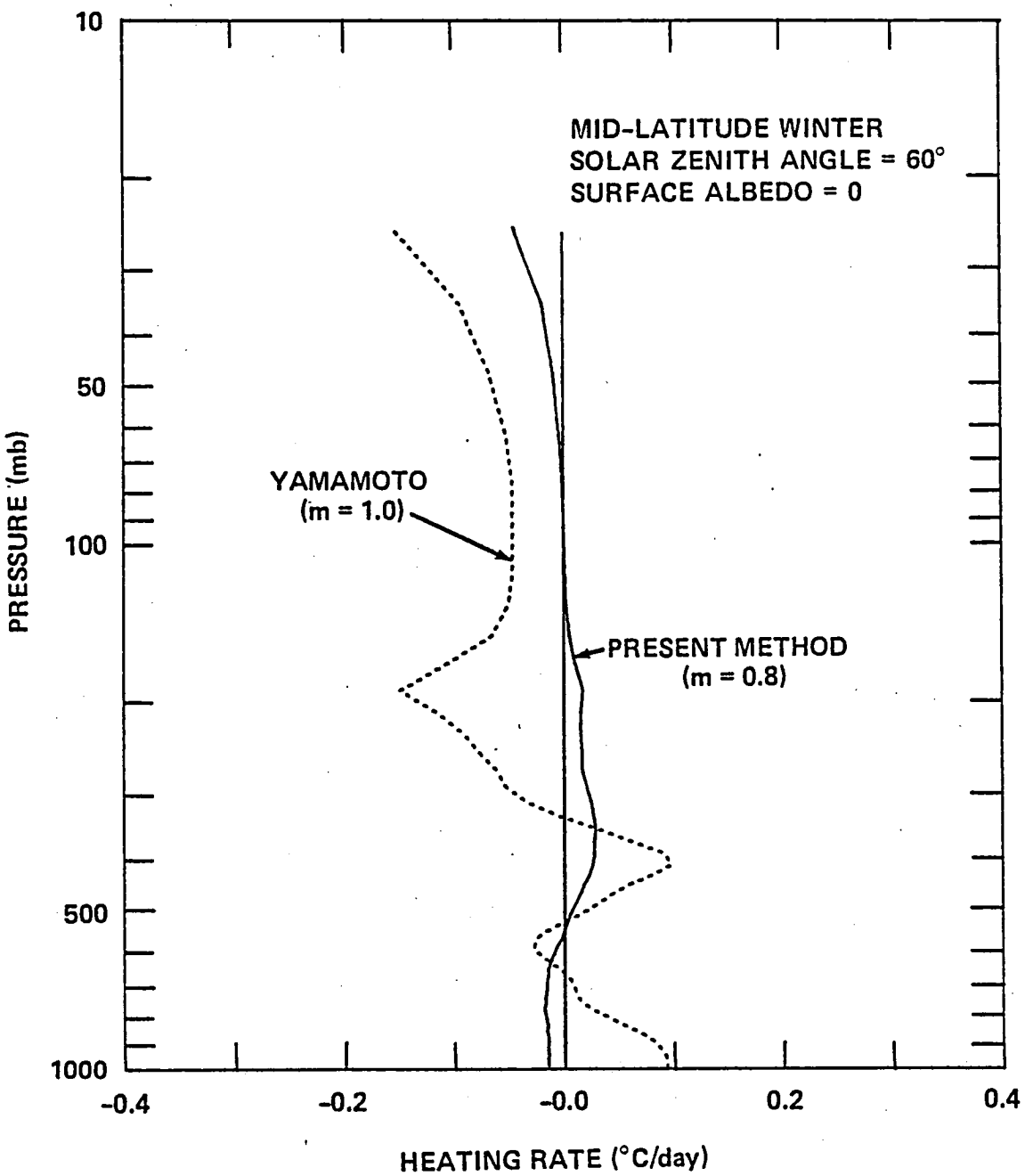
MID-LATITUDE WINTER
SOLAR ZENITH ANGLE = 60°
SURFACE ALBEDO = 0
YAMAMOTO
(m = 1.0)
PRESENT METHOD
(m = 0.8)
PRESSURE (mb)
10
50
100
500
1000
-0.4
-0.2
-0.0
0.2
0.4
HEATING RATE (°C/day)

Fig. 4

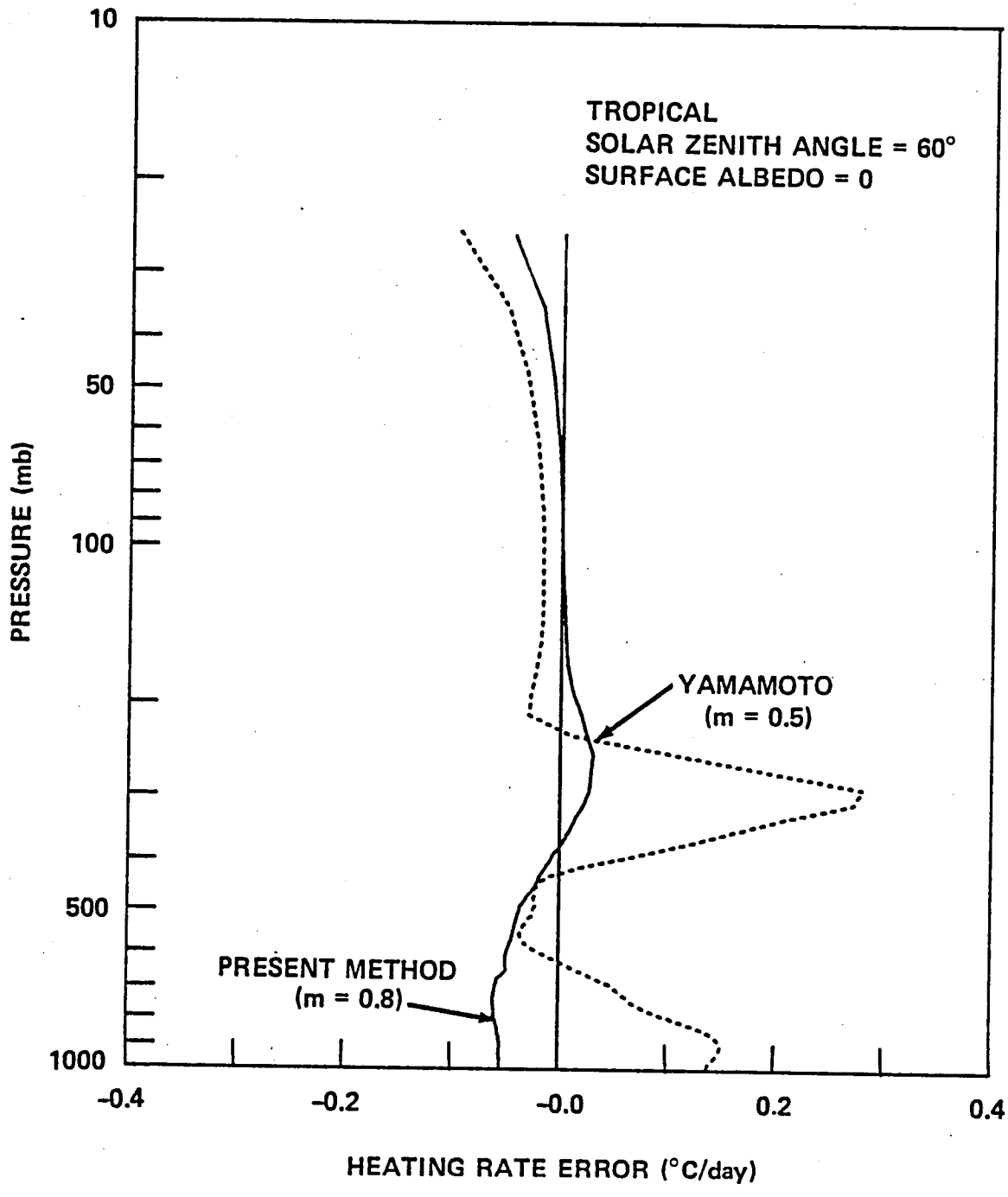
10
50
100
500
1000
PRESSURE (mb)
TROPICAL
SOLAR ZENITH ANGLE = 60°
SURFACE ALBEDO = 0
YAMAMOTO
(m = 0.5)
PRESENT METHOD
(m = 0.8)
-0.4
-0.2
-0.0
0.2
0.4
HEATING RATE ERROR (°C/day)

Fig. 5

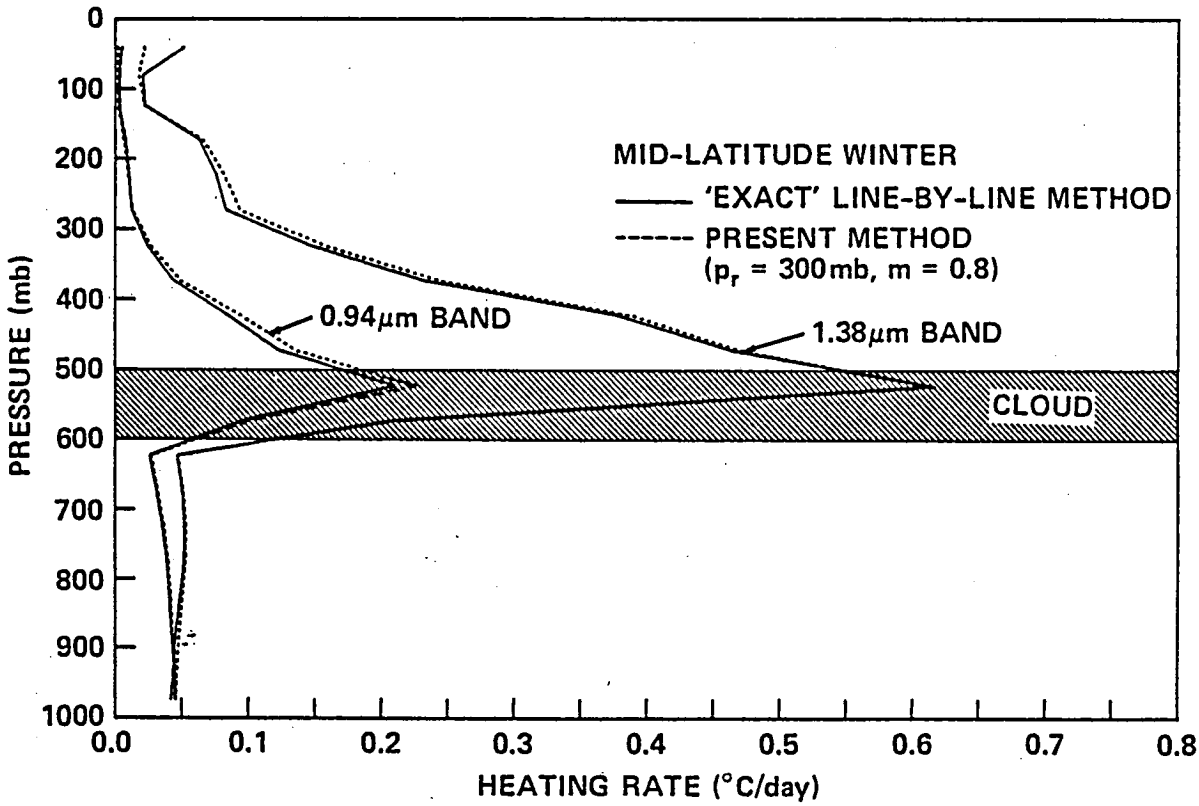

Fig. 6

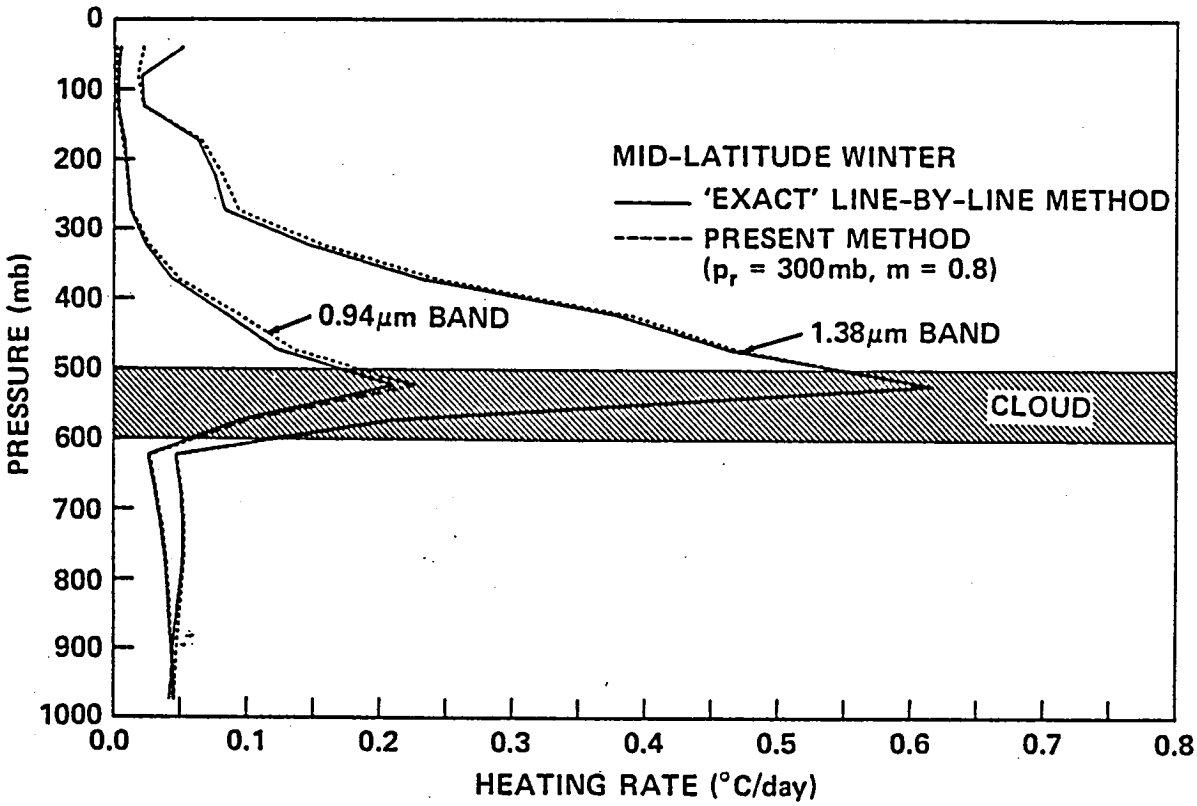

Fig. 6

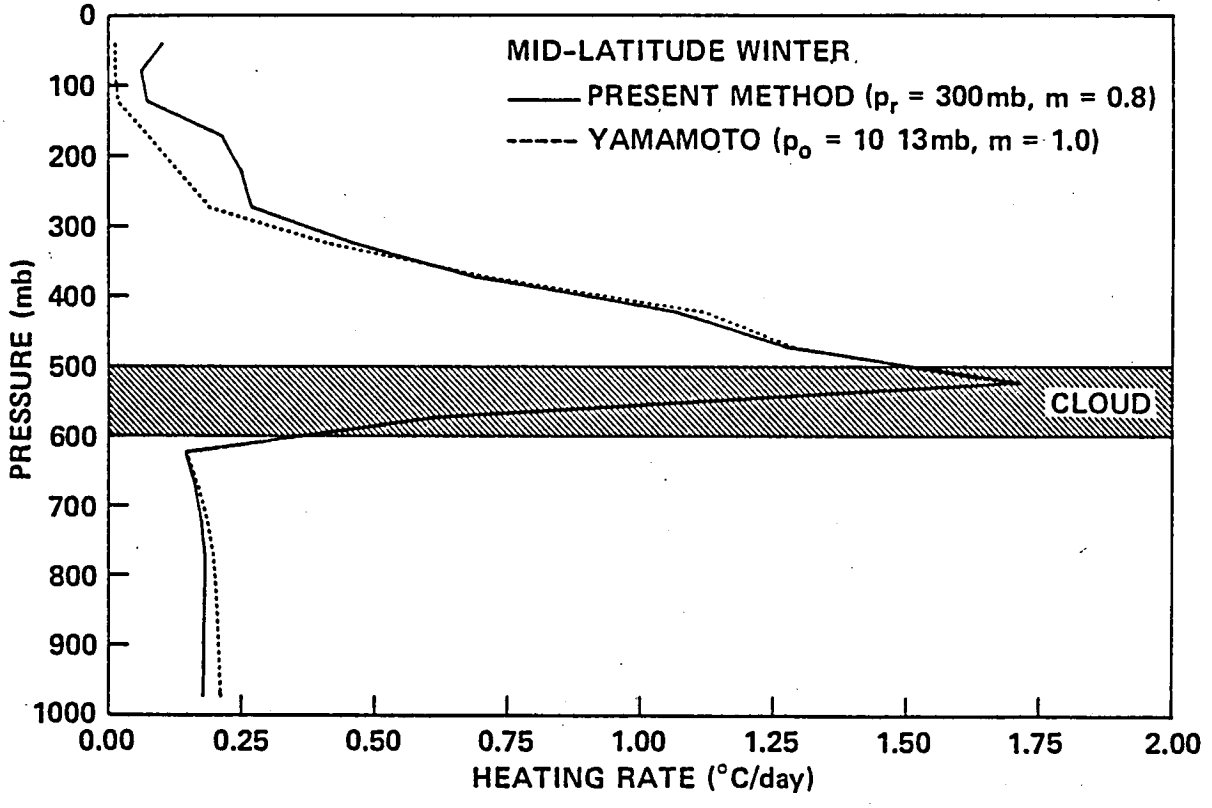
MID-LATITUDE WINTER
PRESENT METHOD (p_r = 300mb, m = 0.8)
YAMAMOTO (p_o = 10 13mb, m = 1.0)
CLOUD
PRESSURE (mb)
0
100
200
300
400
500
600
700
800
900
1000
0.00
0.25
0.50
0.75
1.00
1.25
1.50
1.75
2.00
HEATING RATE (°C/day)

Fig. 7

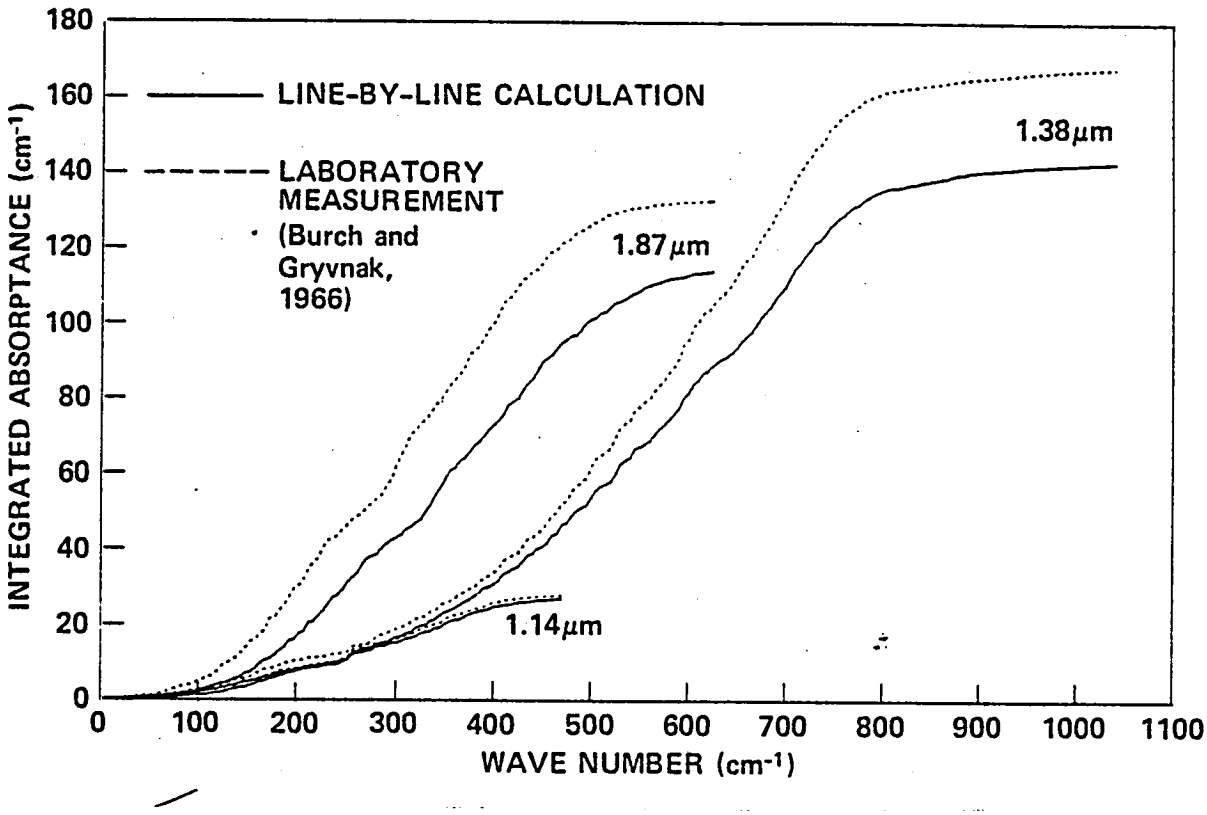
INTEGRATED ABSORPTANCE (cm⁻¹)
WAVE NUMBER (cm⁻¹)
LINE-BY-LINE CALCULATION
LABORATORY MEASUREMENT (Burch and Gryvnak, 1966)
1.38μm
1.87μm
1.14μm
0
20
40
60
80
100
120
140
160
180
0
100
200
300
400
500
600
700
800
900
1000
1100

Fig. 8